Quantification of Mitral Valve Morphology with Three-dimensional Echocardiography: Can Measurement Lead to Better Management?

Alex Pui-Wai Lee[a], MBChB, Fang Fang[a], MD, PhD, Chun-Na Jin[a], MD, PhD, Kevin Ka-Ho Kam[a], MBChB, Gary K.W. Tsui[c], PhD, Kenneth K.Y. Wong[c], PhD, Jen-Li Looi[d], MBChB, Randolph H.L. Wong[b], MBChB, Song Wan[b], MD, PhD, Jing Ping Sun, MD, Malcolm J. Underwood, MD, Cheuk-Man Yu[a], MD

[a] Division of Cardiology, Li Ka Shing Institute of Health Sciences, Department of Medicine and Therapeutics, Prince of Wales Hospital, The Chinese University of Hong Kong

[b] Division of Cardiothoracic Surgery, Department of Surgery, Prince of Wales Hospital, The Chinese University of Hong Kong

[c] Department of Computer Science, The University of Hong Kong

[d] Department of Cardiology, Middlemore Hospital, Auckland, New Zealand

Short title: MV morphologic quantification by 3D echo

This work is supported by the Research Grant Council General Research Fund (No. 467872)

Correspondence to Alex Pui-Wai Lee, Division of Cardiology, Li Ka Shing Institute of Health Sciences, Department of Medicine and Therapeutics, Prince of Wales Hospital, The Chinese University of Hong Kong. E-mail: alexpwlee@cuhk.edu.hk

Word counts: 5989

Abstract

The mitral valve has complex three-dimensional (3D) morphology and motion. Advance in real-time (RT) 3D echocardiography (3DE) has revolutionized clinical imaging of the MV by providing clinicians realistic visualization of the valve. Thus far, RT3DE of the MV structure and dynamics has adopted an approach that depends largely on subjective and qualitative interpretation of the 3D images of the valve, rather than objective and reproducible measurement. RT3DE combined with image-processing computer techniques provide us precise segmentation and reliable quantification of the complex 3D morphology and rapid motion of the MV. This new approach of imaging may provide additional quantitative descriptions that are useful in diagnostic and therapeutic decision-making. Quantitative analysis of the MV using RT3DE has increased new understanding on the pathologic mechanism of degenerative, ischemic, functional, and rheumatic MV disease. Most recently, 3D morphologic quantification has entered into clinical use to provide more accurate diagnosis of MV diseases and planning of surgery and trans-catheter intervention. Current limitations of this quantitative approach to MV imaging include labor-intensiveness during image segmentation and lack of a clear definition of the clinical significance of many morphologic parameters. This review summarizes the current development and applications of quantitative analysis of the MV morphology using RT3DE.

Keywords: mitral regurgitation, echocardiography, imaging

Introduction

In the last 5 years, advance in real-time (RT) three-dimensional echocardiography (3DE) has revolutionized imaging of the mitral valve (MV). Many studies have shown consistently the superiority of 3D transesophageal echocardiography (TEE) over 2D TEE in visualization of MV morphology.[1] RT3DE has become the imaging modality of choice for guiding MV surgery and catheter-based intervention. Currently, RT3D imaging of the MV involves mainly visualization and qualitative interpretation of volume-rendered images. This "qualitative" approach typically involves few quantitative measurement of MV morphology, and is prone to subjectivity that introduces bias, low reproducibility, and high dependency on imaging expertise.

Quantitative cardiac imaging is of growing importance for several reasons: (1) as imaging becomes more digital, the opportunity will create the need; (2) automated approaches to intervention and surgery design and planning are emerging from the laboratory to enter clinical use; (3) algorithm-driven analysis yields faster and more reproducible results; and (4) a variety of users (e.g. cardiac anesthetists) wants to employ the repeatable methodology offered by quantitative methods. Image-processing tools provide us characterization of complex 3D morphology and motion of the MV. Combined with properties of the imaging modality and knowledge of anatomy, they yield quantitative descriptions that are useful in diagnostic and therapeutic decision-making. This review summarizes the current development and applications of quantitative analysis of the MV morphology using 3DE.

Anatomic consideration

<u>Mitral valve leaflets</u>

The anterior leaflet (AL) is in fibrous continuity with the aortic valve and guards one-third of the anterior mitral annulus. Fine demarcations divide the AL into 3 smaller scallops. The posterior leaflet (PL) has a crescent shape and spans the posterior two-third of the mitral annulus. The 3 scallops of PLs are usually distinct and sometimes separated by prominent cleft-like indentations, which normally never reach the annulus.[2] The two leaflets converge at the anterolateral and posteromedial commissures and maintain a coaptation reserve to prevent mitral regurgitation (MR) during systole,[3]; a coaptation length of 5 mm is considered a minimum to ensure adequate leaflet function.[3] In normal valves, ALs are on average 2.3 times longer and 1.5 times larger than PLs.[4]

Mitral annulus

The mitral annulus is a ring-like structure in continuity with the fibrous skeleton of the heart. Its portion between the central fibrous body and anterolateral commissure is in continuity with the aorto-mitral curtain. The inter-commissural width of annulus is normally longer than the antero-posterior diameter, giving the annulus an elliptical shape. The surface area of both leaflets taken together was 140% of the annular area, indicating a large natural surplus of leaflet surfaces to cover the mitral orifice in normal valves.[4]

Subvalvular apparatus

The chordae tendineae are of 3 types: primary, secondary, and tertiary. Primary chordae arise from the papillary muscles and fan out to anchor the edge of both leaflets to prevent leaflets prolapse. Secondary chordae are usually thicker and lesser in number and arise from papillary muscle tips to attach to the ventricular side of the leaflet body. Tertiary chordae arise from ventricular wall and attached to the ventricular side of PL close to the annulus. The chordae tendineae can be pathologically elongated or ruptured, leading to significant MR. In a dilated or distorted left ventricle, the outwardly displaced ventricular wall pulls the chordae apically and posteriorly, tethering the leaflets and resulting in functional MR.[5]

Technology of real-time 3D echocardiography

Prior to the development of matrix-array transducers, reconstruction of the MV was primarily based on a stack of sequentially-scanned 2D images acquired manually or mechanically.[1] Previous techniques produced questionable image quality due to motion artifacts, under-sampling, and noisy signals.[1] Advances in technology have allowed miniaturization of matrix-array transducers, which was achieved by fitting thousands of fully sampled elements into the tip of the 3DE transducer, which not only circumvents the reconstruction issues but also facilitates the visualization of geometry (3D) and motion (4D) of the heart in vivo.

3DE image acquisition of the MV for quantitative analysis is usually performed in the apical 4-chamber views on transthoracic echocardiography, or in mid-esophageal views on TEE.[6] There are generally 2 approaches to 3DE data set acquisition: (1) RT or live 3D imaging and (2) gated acquisition with non-RT reconstruction. In live 3D imaging, a volumetric data set of a relatively narrow pyramidal sector is acquired and displayed in RT. Live imaging is generally a frame-rate of display >20 frames per second, and preferably >30 frames per second. In ECG-gated 3DE acquisition, pyramidal data sets of 4-6 consecutive heartbeats are merged together to obtain a wider volumetric image that is displayed offline. Choice of the mode of imaging is a trade-off between frame-rate, image quality, size of the field-of-view, and image processing time (RT or non-RT). Recently, high volume-rate 3D ultrasound imaging allows volumetric region being imaged to be sparsely sub-sampled by scanning beams, with spatial locations between beams filled in with interpolated values or interleaved with acquired data from other 3D scanning intervals.[7] A full-volume RT3DE data set can then be obtained in a single heartbeat, which is particularly useful when imaging patients with arrhythmias.

Computer techniques for segmentation of mitral valve

The full volumetric data sets acquired by RT3DE are processed within the computer memory and then be three-dimensionally rendered to the computer screen. Then, an optimal view is selected to allow the most favorable segmentation of the image. In computer vision, segmentation is the process that partitions an object into various regions based on their similarities. These similar regions are grouped into a set of pixels (2D) or voxels (3D), which exhibit similar distinguishable characteristics such as gray-level intensity, texture, edge information, etc. The segmented regions could then be taken to quantify the relevant morphological parameters of a structure, the MV for instance, manually or automatically. Currently, the two most commonly used software systems for MV analysis are the Mitral Valve Navigator[A.I.] (MVN[A.I.]; previous versions were called MVQ) (Philips Healthcare, Inc., Andover, MA, USA) and the 4D-MV Assessment (TomTec Imaging Systems GmbH, Munich, Germany).[8, 9] These software packages allow manual or semi-automatic detection of major anatomic landmarks with subsequent surface modeling using a geometric mesh. Morphological quantification of MV can be computed according to the final model (Figure 1). On the other hand, fully automated extraction of morphological parameters remains challenging because signal dropouts, speckle noise, and low tissue contrasts currently limit the quality of RT3DE image, and there is a wide variety of normal and pathological MV geometry. It is now possible to have the annular and leaflet geometry and their motion dynamics quantitatively analyzed using RT3DE with minimal human intervention (Figure 2).[10-12] Nevertheless, without prior knowledge and human input, automatic segmentation of the coaptation zone, scallops,[13] chordae tendineae[14] and papillary muscles[15] remains difficult mainly because RT3DE of these structures has even lower signal-to-noise ratio (i.e. blurrier).

Mitral valve pathophysiology: Lessons learnt from morphologic quantification using 3D echocardiography

Degenerative mitral regurgitation

3DE shows that the mitral annulus has a non-planar hyperbolic paraboloid configuration analogous to a saddle.[16] The annular height-to-width ratio (AHCWR) of this saddle-shape is consistent across mammalian species suggesting an evolutionary advantage.[17] RT3DE-derived computational model shows that saddle-shaped annulus may offer extra mechanical support by adding curvature to leaflet surface.[17] The minimum leaflet stress happened when the AHCWR is in the range of 15% to 25%.[17] In human, we recently undertook a quantitative RT3DE study in patients with MV prolapse (MVP) with a wide spectrum of MR severity to characterize the link between MV morphology and MR severity. For the first time in humans, we demonstrated that annular flattening is strongly associated with progressive leaflet billowing, higher frequencies of chordal rupture, and greater effective regurgitant orifices (ERO) (Figure 3). The lower limit of AHCWR in healthy population appears to be 15%, and a ratio <15% is strongly associated with moderate or severe MR among patients with MVP. Importantly, annular height and AHCWR are reduced even in patients with MVP and no or mild MR, suggesting the possibility of primary annular abnormality. Such annular flattening was not observed in patients with organic MR due to nonprolapse leaflet pathologies.[4] This study, together with other quantitative RT3DE studies of annular dynamics,[18, 19] supports annular flattening as a novel mechanism in the pathogenesis of degenerative MR.[4] From the surgical point of view, MV repair with saddle-shaped annuloplasty ring allows a better leaflet coaptation by not hoisting the papillary muscles towards the posterior annulus.[20, 21] A quantitative RT3DE study performed by Otani et al showed that the nonprolapsed MV leaflets are often apically tethered as a result of left ventricular dilatation attributed to primary MVP-associated MR, and that secondary tethering further exacerbates malcoaptation and contributes to a vicious cycle begetting more MR (Figure 4B).[22] In P2 prolapse, AL tenting volume shows good correlations with left ventricular midsystolic volume and papillary muscle displacement. Multivariate analysis identified both leaflet tenting volume and prolapse volume as independent contributors to MR vena contracta area. These findings would suggest a pathophysiologic rationale for early surgical repair.

<u>Functional or ischemic mitral regurgitation</u>

Functional MR can be defined as MR secondary to left ventricular remodeling in the absence of primary abnormality of the MV (Figure 4C). Leaflet malcoaptation in functional MR is contributed by annular flattening and dilatation,[23] leaflet tethering,[24] reduced rate of rise of left ventricular pressure, as well as systolic dysschrony.[25, 26] RT3DE with quantitative software that manually or semi-automatically track the annular motions has been used by several researchers to study the annular mechanism of functional MR.[18, 19, 27-29] Both Grewal et al[18] and Levack et al[19] found that ischemic annuli are less dynamic than normal, with significantly diminished area contraction, antero-posterior diameter shortening, and saddle-shape accentuation during systole.

Topilsky et al studied in detail the relationship between phasic changes of annular geometry and ERO. Their study showed that different mechanisms contribute to different systolic phases of functional MR, with inadequate early-systolic annular contraction and saddle-shape accentuation determining early-systolic ERO, whereas asymmetric papillary tips movement determining mid- and late-systolic ERO.[27] Differences in MV geometry are observed between asymmetric and symmetric tethering patterns in ischemic MR. For the same degree of tethering, an asymmetric pattern is associated with increased MR severity.[30] RT3DE was also used to measure the surface area of mitral leaflets and discovered that the leaflets may enlarge in adaptation to chronic tethering secondary to left ventricular remodeling due to ischemia/infarction,[31-33] dilated cardiomyopathy,[32] and chronic aortic regurgitation.[34] These observations challenge the current concepts relating functional MR solely to LV remodeling. RT3DE may be the ideal method to noninvasively monitor and understand this leaflet adaptive process, potentially lead to new therapeutic measures to prevent functional MR.

<u>Rheumatic mitral valve disease</u>

In rheumatic mitral stenosis (MS), MV orifice area measured by 3D planimetry is more accurate than 2D planimetry and Doppler assessment.[35] Direct visualization of the MV commissures by 3DE allows morphological evaluation of commissural fusion[36] and calcification,[37] which was underestimated by 2DE in about a fifth of patients.[38] RT3DE revealed that valve shape, not just the size of the orifice, has a potential impact on the flow dynamics across a valve.[39] The coefficient of contraction (=effective/anatomic orifice area) and the related net pressure loss are importantly affected by leaflet geometry in patients with MS. With the use of 3DE and stereolitography, Gilon et al. had confirmed that variations in the 3D geometry of the MV led to varying pressure gradients that were up to 40% higher for the flattest valves for the same anatomic area and flow rate compared with “funnel” shaped valves.[39] Their findings suggested that morphological quantification could address uniquely 3D questions to provide insight into the relations between cardiac structure, pressure, and flows. Areas of the annulus and the anterior and PLs were larger in rheumatic MR than in normal controls (Figure 4D). A large antero-posterior annulus diameter and small PL angle were independently associated with rheumatic MR severity.[40] Morphological quantification of the LV and subvalvular apparatus found that misalignment of the papillary muscles and a narrowed interchordal angle also contribute to rheumatic MR.[41] Valve repair of rheumatic MR is more challenging when leaflet retraction coexists with misalignment of papillary muscles, and morphological quantification will be helpful to guide valve repair, if contemplated.

Mitral-aortic valve coupling

The morphology and function of mitral and aortic annuli are interdependent through their fibrous connection, a phenomenon known as mitral-aortic coupling (MAC).[42] MAC may be an integral part of normal cardiac physiology.[43] Importantly, pathology or surgery of MV may affect the aortic valve, and vice versa, through MAC. RT3DE has allowed non-invasive assessment of MAC in normal,[44] degenerative MVP, and after annuloplasty.[45] Mitral annuloplasty not only reduces systolic contraction of mitral annulus area, but also affect the normal annular dynamics of the untreated aortic valve. Tsang et al.[46] recently demonstrated that aortic stenosis can affect the MV due to calcification of the aorto-mitral curtain. These results have important implications when planning intervention and when developing new annuloplasty rings with the goal of preserving physiologic MAC.

Current clinical application of morphological quantification of mitral valve

Diagnosis of mitral valve prolapse

Diagnosis of MVP on 2D echocardiography is defined as leaflet displacement ≥2mm above the annular plane in parasternal long-axis view. This definition takes into consideration the saddle-shape of annulus, which explains why MVP can be over-diagnosed if apical 4-chamber view is used for its diagnosis.[47] In the parasternal long-axis plane, however, the most frequently imaged segments are A2 and P2, making the diagnosis of prolapse of other segments challenging on 2DE. Color-coded parametric 3D display of the MV provides information of the contour and displacement of all 6 segments of the leaflets relative to the saddle-shaped annulus, and may improve diagnostic accuracy (Figure 2 and 4B).[4, 48, 49] In addition, 3D MV quantification could allow us to better recognize secondary lesions of MVP such as mitral clefts (defined as extending ≥50% of leaflet height) and subclefts (<50% of leaflet height).[50]

Surgical planning for mitral valve repair

Quantitative analysis of the MV could objectively identify repairable disease and guide surgical intervention. Morphological analysis in assessing MV billowing revealed significant quantifiable differences between normal, fibroelastic deficiency, and Barlow's disease patients.[49] Billowing height with a cutoff value of 1.0 mm distinguishes MVP from normal subjects, and billowing volume with a cutoff value 1.15 mL differentiates between fibroelastic deficiency (simpler repair expected) and Barlow's disease (complex repair expected). Combining quantitative and qualitative RT3DE imaging of the MV improves repair rates. Complexity of degenerative repair can be predicted from quantifiable parameters including commissural width and number of prolapsing segments.[51]

Functional MR repair is associated with high rates of recurrence.[25] Understanding the coaptation deficiency preoperatively, and modeling the coaptation anatomy likely to result after a certain repair strategy remains the ultimate promise of 3D imaging. Quantitative 3DE allows precise calculation of the leaflets angles, tenting volume, leaflet area, and interpapillary muscles distance.[52] Tenting area and A2 bending angle are both independently correlated with complexity of functional MR repair.[51] In patients undergoing undersized annuloplasty for ischemic MR, a PL angle≥45 degrees predicts poor post-annuloplasty outcome.[53] In patients with dilated cardiomyopathy undergoing annuloplasty for functional MR, we demonstrated that postoperative mitral competence is highly dependent on distal AL mobility. For distal AL angle>25°, the positive and negative predictive values in predicting recurrent MR are 82%, and 93%, respectively.[5] While 2DE was used to measure the leaflet tethering angles, 3DE may provide more precise measurements (Figure 5). Fattouch et al. reported that by modeling the 3D anatomy of subvalvular apparatus preoperatively as a “truncated cone”, new position of surgically relocated papillary muscles head desirable to achieve adequate leaflet coaptation can be pre-calculated.[54]

Guiding of transcatheter mitral valve intervention and development of new devices

During percutaneous transcatheter mitral valvotomy (PTMV), Anwar et al proposed a semi-quantitative RT3DE score with higher points indicating increasing MV thickness, immobility, calcification, and subvalvular involvement. At 1 year after PTMV, the rate of re-stenosis, significant MR or re-intervention in patients with favorable RT3DE score was 17%, but 48% by Wilkins's score. Accordingly, the use of RT3DE score may identify more patients with unsuitable anatomy for PTMV.[55]

Accurate assessment of gap and width as well as billowing height and volume is necessary for selection of potential candidates for percutaneous MV repair using the MitraClip system.[56] Besides the site of prolapse, 3D TEE could provide a more precise quantification of prolapse gap and width than 2D imaging (Figure 6).[57] Post-intervention, 3DE quantification of the area of the double-orifices is feasible to assess MS in adjunct to Doppler assessment.[58]

Limitation and future direction

The main limitation of quantitative MV imaging is that the procedure involved in segmentation of the valve is currently too time-consuming to be incorporated into routine clinical use. Moreover, manual input to define anatomic landmarks of the MV tends to introduce bias, measurement errors and variability. Automated morphological quantification using intelligent algorithms for anatomic recognition will likely improve efficiency and reproducibility of the MV modeling process to a degree optimal for day-to-day diagnostic use. Advances in hardware and software leading to improvement in the 3DE image quality will also enhance the robustness of the segmentation process. Furthermore, morphologic segmentation provides the biomechanical basis for novel application of computer modeling and simulation techniques that will allow studying the MV in even more detail.[59] More importantly, future studies should aim to identify which of these numerous parameters are of clinical significance, provide cut-off values for decisions making, and define the impact on patient outcome.

Conclusion

"You can't manage what you don't measure." — It is an old business management adage that may also be true in understanding and managing such complex diseases as those of the MV. Recent advance in surgical and transcathether intervention techniques for MV diseases has created an unprecedented clinical need to describe the MV morphology and function in precise and quantifiable details. The question of "what to measure and how?" should be answered by future studies. Quantitative dynamic 3D imaging techniques such as RT3DE of the MV will likely become an important tool to guide decision making for the most appropriate management of individual patents to achieve the best outcome.

References

1. Hung J, Lang R, Flachskampf F, Shernan SK, McCulloch ML, Adams DB, et al. 3D echocardiography: a review of the current status and future directions. *Journal of the American Society of Echocardiography : official publication of the American Society of Echocardiography* 2007;**20**:213-233.

2. Looi JL, Lee AP, Wan S. Diagnosis of cleft mitral valve using real-time 3-dimensional transesophageal echocardiography. *International journal of cardiology* 2013:1-3.

3. Silbiger JJ, Bazaz R. Contemporary insights into the functional anatomy of the mitral valve. *Am Heart J* 2009;**158**:887-895.

4. Lee AP, Hsiung MC, Salgo IS, Fang F, Xie JM, Zhang YC, et al. Quantitative analysis of mitral valve morphology in mitral valve prolapse with real-time 3-dimensional echocardiography: importance of annular saddle shape in the pathogenesis of mitral regurgitation. *Circulation* 2013;**127**:832-841.

5. Lee AP, Acker M, Kubo SH, Bolling SF, Park SW, Bruce CJ, et al. Mechanisms of recurrent functional mitral regurgitation after mitral valve repair in nonischemic dilated cardiomyopathy: importance of distal anterior leaflet tethering. *Circulation* 2009;**119**:2606-2614.

6. Lang RM, Badano LP, Tsang W, Adams DH, Agricola E, Buck T, et al. EAE/ASE recommendations for image acquisition and display using three-dimensional

echocardiography. *Journal of the American Society of Echocardiography : official publication of the American Society of Echocardiography* 2012;**25**:3-46.

7. Badano LP, Muraru D, Rigo F, Del Mestre L, Ermacora D, Gianfagna P, et al. High volume-rate three-dimensional stress echocardiography to assess inducible myocardial ischemia: a feasibility study. *Journal of the American Society of Echocardiography : official publication of the American Society of Echocardiography* 2010;**23**:628-635.

8. Jassar AS, Brinster CJ, Vergnat M, Robb JD, Eperjesi TJ, Pouch AM, et al. Quantitative mitral valve modeling using real-time three-dimensional echocardiography: technique and repeatability. *Ann Thorac Surg* 2011;**91**:165-171.

9. Andrawes MN, Feinman JW. 3-dimensional echocardiography and its role in preoperative mitral valve evaluation. *Cardiol Clin* 2013;**31**:271-285.

10. Pouch A, Wang H, Takabe M, Jackson B, Gorman III J, Gorman R, et al. Fully automatic segmentation of the mitral leaflets in 3D transesophageal echocardiographic images using multi-atlas joint label fusion and deformable medial modeling. *Medical image analysis* 2014;**18**:118-129.

11. Sprouse C, Mukherjee R, Burlina P. Mitral Valve Closure Prediction with 3D Personalized Anatomical Models and Anisotropic Hyperelastic Tissue Assumptions. 2013.

12. Schneider R, Burke W, Marx G, Nido P, Howe R. Modeling Mitral Valve Leaflets from Three-Dimensional Ultrasound. In: Metaxas D, Axel L, eds. Functional Imaging and Modeling of the Heart: Springer Berlin Heidelberg; 2011:215-222.

13. Ahmed S, Nanda NC, Miller AP, Nekkanti R, Yousif AM, Pacifico AD, et al. Usefulness of Transesophageal Three-Dimensional Echocardiography in the Identification of Individual Segment/Scallop Prolapse of the Mitral Valve. *Echocardiography* 2003;**20**:203-209.

14. Kanik J, Mansi T, Voigt I, Sharma P, Ionasec RI, Comaniciu D, et al. Automatic Personalization of the Mitral Valve Biomechanical Model Based on 4D Transesophageal Echocardiography. In: Statistical Atlases and Computational Models of the Heart. Imaging and Modelling Challenges: Springer; 2014:162-170.

15. Voigt I, Mansi T, Ionasec R, Mengue E, Houle H, Georgescu B, et al. Robust Physically-Constrained Modeling of the Mitral Valve and Subvalvular Apparatus. In: Fichtinger G, Martel A, Peters T, eds. Medical Image Computing and Computer-Assisted Intervention – MICCAI 2011: Springer Berlin Heidelberg; 2011:504-511.

16. Levine Ra, Handschumacher MD, Sanfilippo aJ, Hagege aa, Harrigan P, Marshall JE, et al. Three-dimensional echocardiographic reconstruction of the mitral valve, with implications for the diagnosis of mitral valve prolapse. *Circulation* 1989;**80**:589-598.

17. Salgo IS. Effect of Annular Shape on Leaflet Curvature in Reducing Mitral Leaflet Stress. *Circulation* 2002;**106**:711-717.

18. Grewal J, Suri R, Mankad S, Tanaka A, Mahoney DW, Schaff HV, et al. Mitral annular dynamics in myxomatous valve disease: new insights with real-time 3-dimensional echocardiography. *Circulation* 2010;**121**:1423-1431.

19. Levack MM, Jassar AS, Shang EK, Vergnat M, Woo YJ, Acker MA, et al. Three-dimensional echocardiographic analysis of mitral annular dynamics: implication for annuloplasty selection. *Circulation* 2012;**126**:S183-188.

20. Jensen MO, Jensen H, Levine Ra, Yoganathan AP, Andersen NT, Nygaard H, et al. Saddle-shaped mitral valve annuloplasty rings improve leaflet coaptation geometry. *The Journal of thoracic and cardiovascular surgery* 2011;**142**:697-703.

21. Jensen MO, Jensen H, Smerup M, Levine RA, Yoganathan AP, Nygaard H, et al. Saddle-shaped mitral valve annuloplasty rings experience lower forces compared with flat rings. *Circulation* 2008;**118**:S250-255.

22. Otani K, Takeuchi M, Kaku K, Haruki N, Yoshitani H, Eto M, et al. Evidence of a Vicious Cycle in Mitral Regurgitation With Prolapse: Secondary Tethering Attributed to Primary Prolapse Demonstrated by Three-Dimensional Echocardiography Exacerbates Regurgitation. *Circulation* 2012;**126**:S214-S221.

23. Watanabe N, Ogasawara Y, Yamaura Y, Wada N, Kawamoto T, Toyota E, et al. Mitral annulus flattens in ischemic mitral regurgitation: geometric differences between inferior and anterior myocardial infarction: a real-time 3-dimensional echocardiographic study. *Circulation* 2005;**112**:I458-462.

24. Watanabe N, Ogasawara Y, Yamaura Y, Kawamoto T, Toyota E, Akasaka T, et al. Quantitation of mitral valve tenting in ischemic mitral regurgitation by transthoracic real-time three-dimensional echocardiography. *J Am Coll Cardiol* 2005;**45**:763-769.

25. Levine Ra, Schwammenthal E. Ischemic mitral regurgitation on the threshold of a solution: from paradoxes to unifying concepts. *Circulation* 2005;**112**:745-758.

26. Liang YJ, Zhang Q, Fang F, Lee AP, Liu M, Yan BP, et al. Incremental value of global systolic dyssynchrony in determining the occurrence of functional mitral regurgitation in patients with left ventricular systolic dysfunction. *Eur Heart J* 2013;**34**:767-774.

27. Topilsky Y, Vaturi O, Watanabe N, Bichara V, Nkomo VT, Michelena H, et al. Real-time 3-dimensional dynamics of functional mitral regurgitation: a prospective quantitative and mechanistic study. *J Am Heart Assoc* 2013;**2**:e000039.

28. Khabbaz KR, Mahmood F, Shakil O, Warraich HJ, Gorman JH, Gorman RC, et al. Dynamic 3-dimensional echocardiographic assessment of mitral annular geometry in patients with functional mitral regurgitation. *The Annals of thoracic surgery* 2013;**95**:105-110.

29. Bartels K, Thiele RH, Phillips-Bute B, Glower DD, Swaminathan M, Kisslo J, et al. Dynamic indices of mitral valve function using perioperative three-dimensional transesophageal echocardiography. *J Cardiothorac Vasc Anesth* 2014;**28**:18-24.

30. Zeng X, Nunes MC, Dent J, Gillam L, Mathew JP, Gammie JS, et al. Asymmetric versus Symmetric Tethering Patterns in Ischemic Mitral Regurgitation: Geometric Differences from Three-Dimensional Transesophageal Echocardiography. *J Am Soc Echocardiogr* 2014.

31. Chaput M, Handschumacher MD, Guerrero JL, Holmvang G, Dal-Bianco JP, Sullivan S, et al. Mitral leaflet adaptation to ventricular remodeling: prospective changes in a model of ischemic mitral regurgitation. *Circulation* 2009;**120**:S99-103.

32. Chaput M, Handschumacher MD, Tournoux F, Hua L, Guerrero JL, Vlahakes GJ, et al. Mitral leaflet adaptation to ventricular remodeling: occurrence and adequacy in patients with functional mitral regurgitation. *Circulation* 2008;**118**:845-852.

33. Saito K, Okura H, Watanabe N, Obase K, Tamada T, Koyama T, et al. Influence of chronic tethering of the mitral valve on mitral leaflet size and coaptation in functional mitral regurgitation. *JACC Cardiovasc Imaging* 2012;**5**:337-345.

34. Beaudoin J, Handschumacher MD, Zeng X, Hung J, Morris EL, Levine RA, et al. Mitral Valve Enlargement in Chronic Aortic Regurgitation as a Compensatory Mechanism to Prevent Functional Mitral Regurgitation in the Dilated Left Ventricle. *Journal of the American College of Cardiology* 2013;**61**:1809-1816.

35. Zamorano J, de Agustín JA. Three-dimensional echocardiography for assessment of mitral valve stenosis. *Current opinion in cardiology* 2009;**24**:415-419.

36. Schlosshan D, Aggarwal G, Mathur G, Allan R, Cranney G. Real-time 3D transesophageal echocardiography for the evaluation of rheumatic mitral stenosis. *JACC. Cardiovascular imaging* 2011;**4**:580-588.

37. Langerveld J, Valocik G, Plokker HW, Ernst SM, Mannaerts HF, Kelder JC, et al. Additional value of three-dimensional transesophageal echocardiography for patients with mitral valve stenosis undergoing balloon valvuloplasty. *J Am Soc Echocardiogr* 2003;**16**:841-849.

38. Messika-Zeitoun D, Brochet E, Holmin C, Rosenbaum D, Cormier B, Serfaty JM, et al. Three-dimensional evaluation of the mitral valve area and commissural opening

before and after percutaneous mitral commissurotomy in patients with mitral stenosis. *Eur Heart J* 2007;**28**:72-79.

39. Gilon D, Cape EG, Handschumacher MD, Jiang L, Sears C, Solheim J, et al. Insights from three-dimensional echocardiographic laser stereolithography. Effect of leaflet funnel geometry on the coefficient of orifice contraction, pressure loss, and the Gorlin formula in mitral stenosis. *Circulation* 1996;**94**:452-459.

40. Song JM, Jung YJ, Jung YJ, Ji HW, Kim DH, Kang DH, et al. Three-Dimensional Remodeling of Mitral Valve in Patients With Significant Regurgitation Secondary to Rheumatic Versus Prolapse Etiology. *American Journal of Cardiology* 2013;**111**:1631-1637.

41. Wong S, French R, Bolson E, McDonald J, Legget M, Sheehan F. Morphologic features of the rheumatic mitral regurgitant valve by three-dimensional echocardiography. *American heart journal* 2001;**142**:897-907.

42. Lansac E, Lim KH, Shomura Y, Goetz Wa, Lim HS, Rice NT, et al. Dynamic balance of the aortomitral junction. *The Journal of Thoracic and Cardiovascular Surgery* 2002;**123**:911-918.

43. Timek TA, Green GR, Tibayan FA, Lai DT, Rodriguez F, Liang D, et al. Aorto-mitral annular dynamics. *Ann Thorac Surg* 2003;**76**:1944-1950.

44. Veronesi F, Corsi C, Sugeng L, Mor-Avi V, Caiani EG, Weinert L, et al. A study of functional anatomy of aortic-mitral valve coupling using 3D matrix transesophageal echocardiography. *Circulation. Cardiovascular imaging* 2009;**2**:24-31.

45. Veronesi F, Caiani EG, Sugeng L, Fusini L, Tamborini G, Alamanni F, et al. Effect of mitral valve repair on mitral-aortic coupling: a real-time three-dimensional transesophageal echocardiography study. *Journal of the American Society of Echocardiography : official publication of the American Society of Echocardiography* 2012;**25**:524-531.

46. Tsang W, Meineri M, Hahn RT, Veronesi F, Shah AP, Osten M, et al. A three-dimensional echocardiographic study on aortic-mitral coupling in transcatheter aortic valve replacement. *Eur Heart J Cardiovasc Imaging* 2013;**14**:950-956.

47. Levine RA, Stathogiannis E, Newell JB, Harrigan P, Weyman AE. Reconsideration of echocardiographic standards for mitral valve prolapse: lack of association between leaflet displacement isolated to the apical four chamber view and independent echocardiographic evidence of abnormality. *J Am Coll Cardiol* 1988;**11**:1010-1019.

48. Addetia K, Mor-Avi V, Weinert L, Salgo IS, Lang RM. A new definition for an old entity: improved definition of mitral valve prolapse using three-dimensional echocardiography and color-coded parametric models. *J Am Soc Echocardiogr* 2014;**27**:8-16.

49. Chandra S, Salgo IS, Sugeng L, Weinert L, Tsang W, Takeuchi M, et al. Characterization of degenerative mitral valve disease using morphologic analysis of real-time three-dimensional echocardiographic images: objective insight into complexity and planning of mitral valve repair. *Circulation. Cardiovascular imaging* 2011;**4**:24-32.

50. La Canna G, Arendar I, Maisano F, Monaco F, Collu E, Benussi S, et al. Real-time three-dimensional transesophageal echocardiography for assessment of mitral valve functional anatomy in patients with prolapse-related regurgitation. *Am J Cardiol* 2011;**107**:1365-1374.

51. Drake DH, Zimmerman KG, Hepner AM, Nichols CD. Echo-Guided Mitral Repair. *Circulation-Cardiovascular Imaging* 2014;**7**:132-141.

52. Fattouch K, Castrovinci S, Murana G, Novo G, Caccamo G, Bertolino EC, et al. Multiplane two-dimensional versus real time three-dimensional transesophageal echocardiography in ischemic mitral regurgitation. *Echocardiography* 2011;**28**:1125-1132.

53. Magne J, Pibarot P, Dagenais F, Hachicha Z, Dumesnil JG, Sénéchal M. Preoperative posterior leaflet angle accurately predicts outcome after restrictive mitral valve annuloplasty for ischemic mitral regurgitation. *Circulation* 2007;**115**:782-791.

54. Fattouch K, Castrovinci S, Murana G, Dioguardi P, Guccione F, Bianco G, et al. Relocation of papillary muscles for ischemic mitral valve regurgitation: the role of three-dimensional transesophageal echocardiography. *Innovations (Phila)* 2014;**9**:54-59.

55. Anwar AM, Attia WM, Nosir YFM, Soliman OII, Mosad Ma, Othman M, et al. Validation of a new score for the assessment of mitral stenosis using real-time three-dimensional echocardiography. *Journal of the American Society of Echocardiography : official publication of the American Society of Echocardiography* 2010;**23**:13-22.

56. Feldman T, Foster E, Glower DD. Percutaneous Repair or Surgery for Mitral Regurgitation. *The New England journal of medicine* 2011:1-12.

57. Izumo M, Shiota M, Kar S, Gurudevan SV, Tolstrup K, Siegel RJ, et al. Comparison of Real-Time Three-Dimensional Transesophageal Echocardiography to Two-Dimensional Transesophageal Echocardiography for Quantification of Mitral Valve Prolapse in Patients With Severe Mitral Regurgitation. *The American Journal of Cardiology* 2013;**111**:588-594.

58. Biaggi P, Felix C, Gruner C, Herzog BA, Hohlfeld S, Gaemperli O, et al. Assessment of mitral valve area during percutaneous mitral valve repair using the MitraClip system: comparison of different echocardiographic methods. *Circ Cardiovasc Imaging* 2013;**6**:1032-1040.

59. Noack T, Kiefer P, Ionasec R, Voigt I, Mansi T, Vollroth M, et al. New concepts for mitral valve imaging. *Ann Cardiothorac Surg* 2013;**2**:787-795.

Figure legends

Figure 1. Computerized segmentation of the MV. (A) Volume-rendered image of MVP. (B) Semi-automatic segmentation of the MV using MVN$^{A.I.}$ (Philips Healthcare) at a systolic frame can be initiated by schematically guided manual marking of 4 annular points and one nadir. (C) The software then traces annulus and leaflets contour to generate a color-coded display, with red indicating leaflet billowing above the annulus plane. Morphologic parameters of the MV are reported on the right. (D) Similar segmentation of a normal MV using 4D-MV Assessment (TomTec).

Figure 2. (A) Segmentation of the annulus/leaflets, and (B) anterior (blue)/posterior (red) leaflets by computer algorithms.

Figure 3. Illustrative examples of MV deformation in MVP. (A) A control subject with a saddle-shaped annulus (AHCWR=23%). (B) A patient with mild MVP and mild MR. RT3DE reveals P2 billowing (arrow). Morphological quantification shows that the saddle shape of annulus decreases (AHCWR=18%), and a light-red hue localized to P2 with a billow volume of 0.2 mL. (C) A patient with chordal rupture, flail P2 and severe MR. The ruptured chord (arrowheads) can be visualized on RT3DE. The annular saddle shape is lost (AHCWR=14%). Leaflet topography shows a deep-red hue at P2, indicating P2 prolapse with a large coaptation gap (asterisk). Leaflet billow volume=0.8 mL. (D) A patient with Barlow's disease severe MR. The annulus is extremely flat (AHCWR=10%), and diffuse deep-red discoloration over multiple scallops, indicating extensive leaflet billowing (billow volume=7.8 mL). Lee AP, et al. Quantitative analysis of mitral valve morphology in mitral valve prolapse with real-time 3-dimensional echocardiography:

importance of annular saddle shape in the pathogenesis of mitral regurgitation. Circulation 2013;127:832-841.[4] Reproduced with permission.

Figure 4. Color-coded topographic display by 4D-MV Assessment (TomTec). (A) Normal MV; (B) Functional MR. Leaflet enlargement is evident. Regions of leaflet tethering is displayed blue (yellow arrow); (C) MVP. Localized P3 prolapse is displaced red (white arrow); secondary AL tethering blue (yellow arrow); (D) Rheumatic MV. Leaflets enlargement and, in this case, diffuse billowing can be seen.

Figure 5. (A) MV geometry measurement in parasternal long-axis view. A, anterior annulus; C, coaptation point; AP, annular diameter; CD, coaptation depth; LA, left atrium; P, posterior annulus; and S, secondary chordae insertion. Tethering of basal AL by secondary chordae can be quantified by the angle between annular plane and AL body (ALA_{base}); tethering of distal AL quantified by the angle between annular plane and a line joining anterior annulus and coaptation point (distal AL angle [ALA_{tip}]). The mobility of PL is quantified by the angle between annular plane and PL (PLA). (B) A patient with functional MR complicating heart failure. Upper panel: TEE long-axis view shows asymmetric tethering of PL (green arrow) and bending of AL body in association with severe eccentric MR. The distal AL seems not tethered, touching the annular plane during systole. Lower panel: 3DE shows tethering of P2 (green arrow). (C) Color-coded topographic display reveals AL tethering limited to the body of the AL (asterisk), hence its bending on 2DE. ALA_{tip} (θ Ant) is small (12.8°), whereas PLA is large (53.4°). ALA_{tip} <25° is predictive of successful repair for nonischemic functional MR by undersized annuloplasty.[5] (D) The post-annuloplasty MV functions as an unicuspid valve but because the AL tip is not tethered, good leaflet coaptation is achieved despite basal

AL tethering (lower panel; note the bending of AL persists). Lee AP, et al. Mechanisms of recurrent functional mitral regurgitation after mitral valve repair in nonischemic dilated cardiomyopathy: importance of distal anterior leaflet tethering. Circulation 2009;119:2606-2614.[5] Modified with permission.

Figure 6. The 3D data set of the MV obtained from 3D-TEE was manually cropped using the plane perpendicular to the MV until the largest cross-sectional prolapse gap and width of the MV were observed. Biaggi P, et al. Assessment of mitral valve area during percutaneous mitral valve repair using the MitraClip system: comparison of different echocardiographic methods. Circ Cardiovasc Imaging 2013;6:1032-1040.[58] Reproduced with permission.

Figures

Figure 1

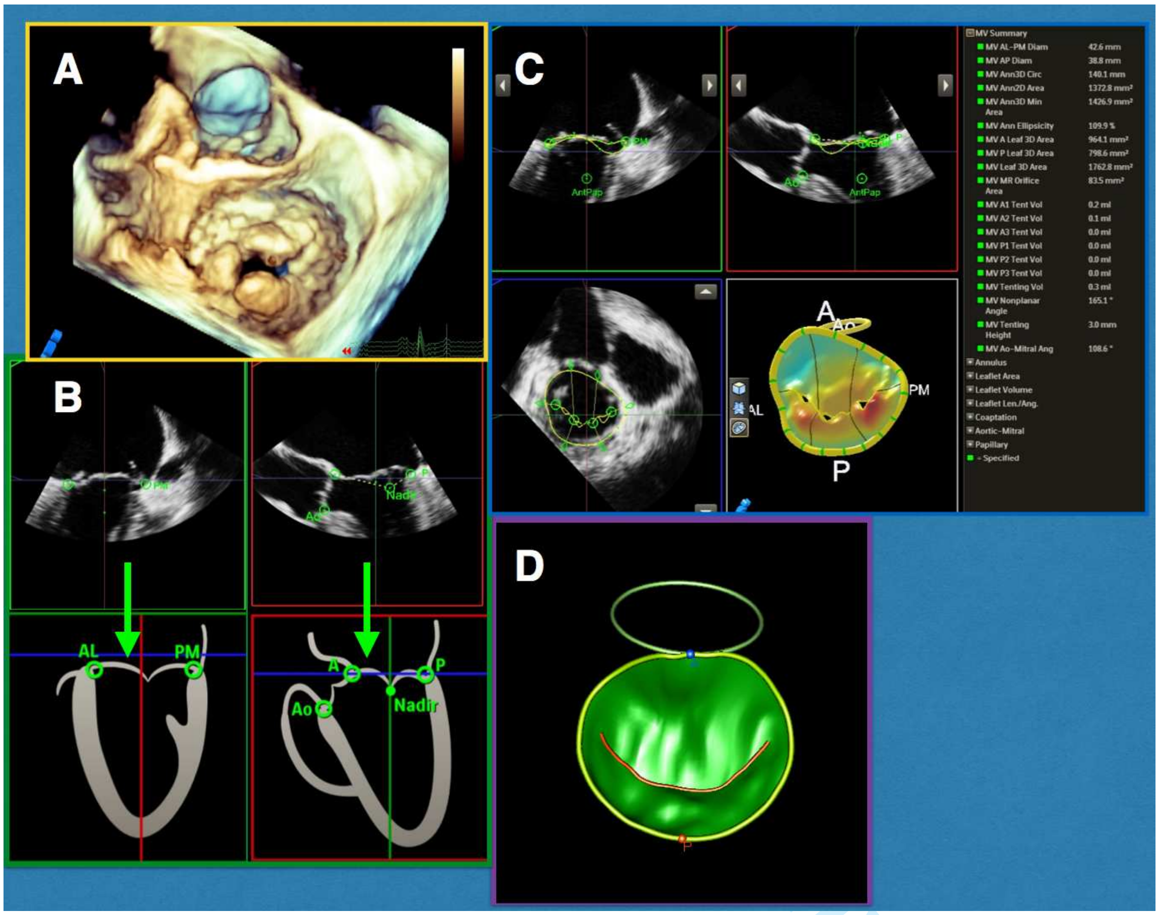

Figure 2

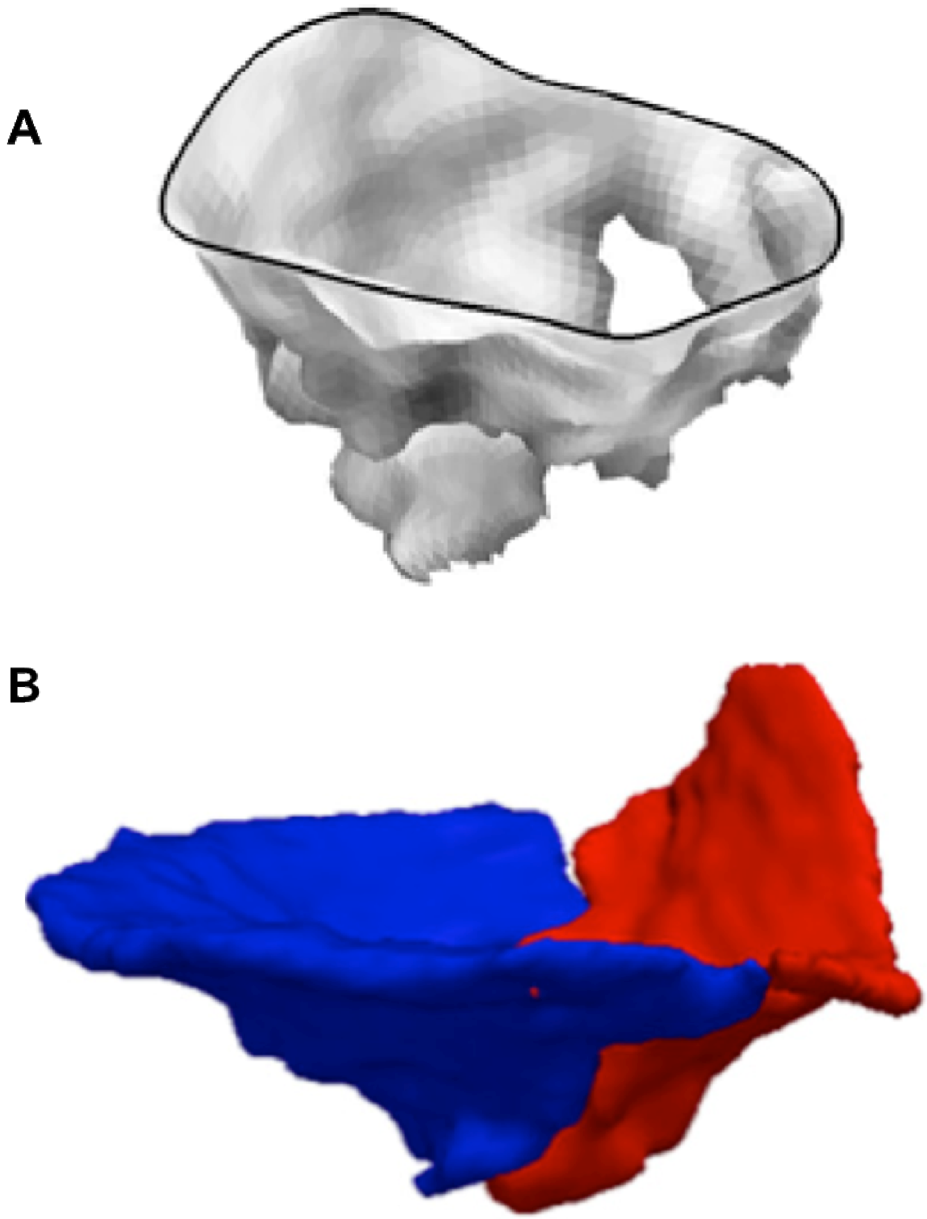

Figure 3

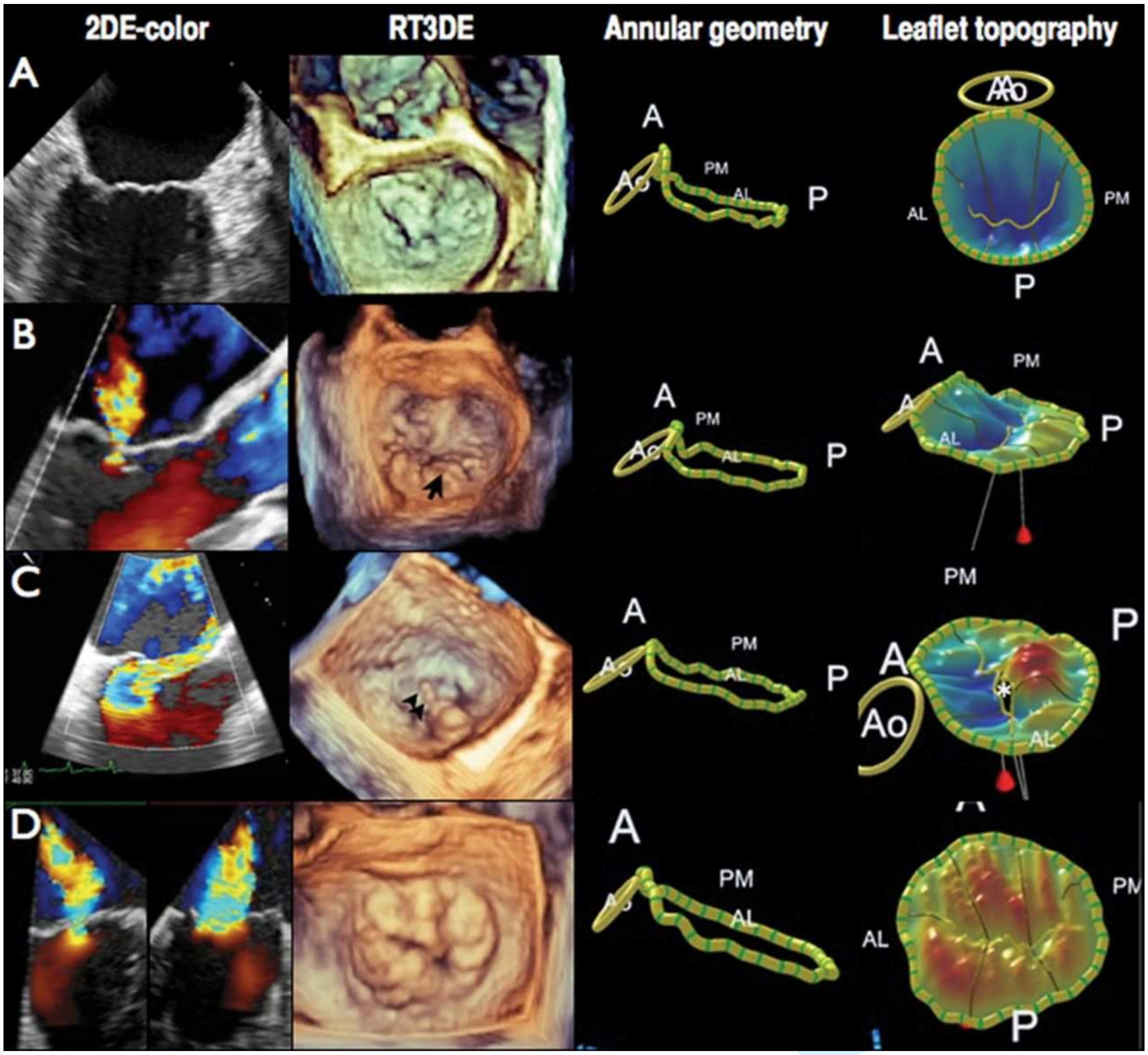
2DE-color
RT3DE
Annular geometry
Leaflet topography
A
B
C
D
A
Ao
PM
AL
P

Figure 4

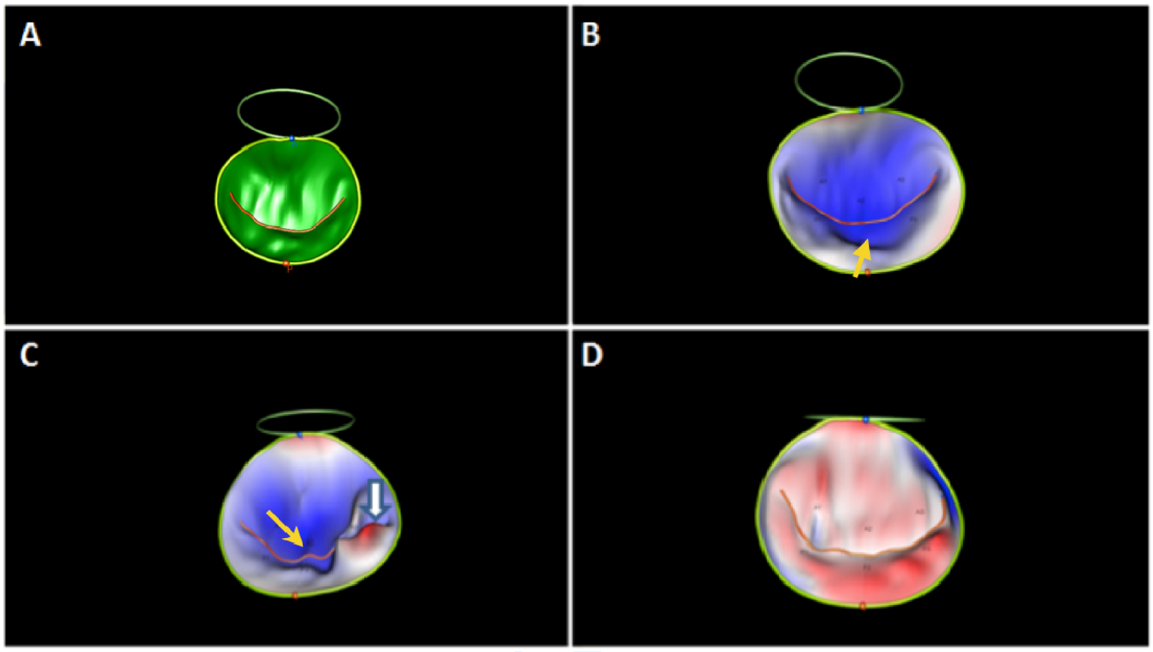

Figure 5

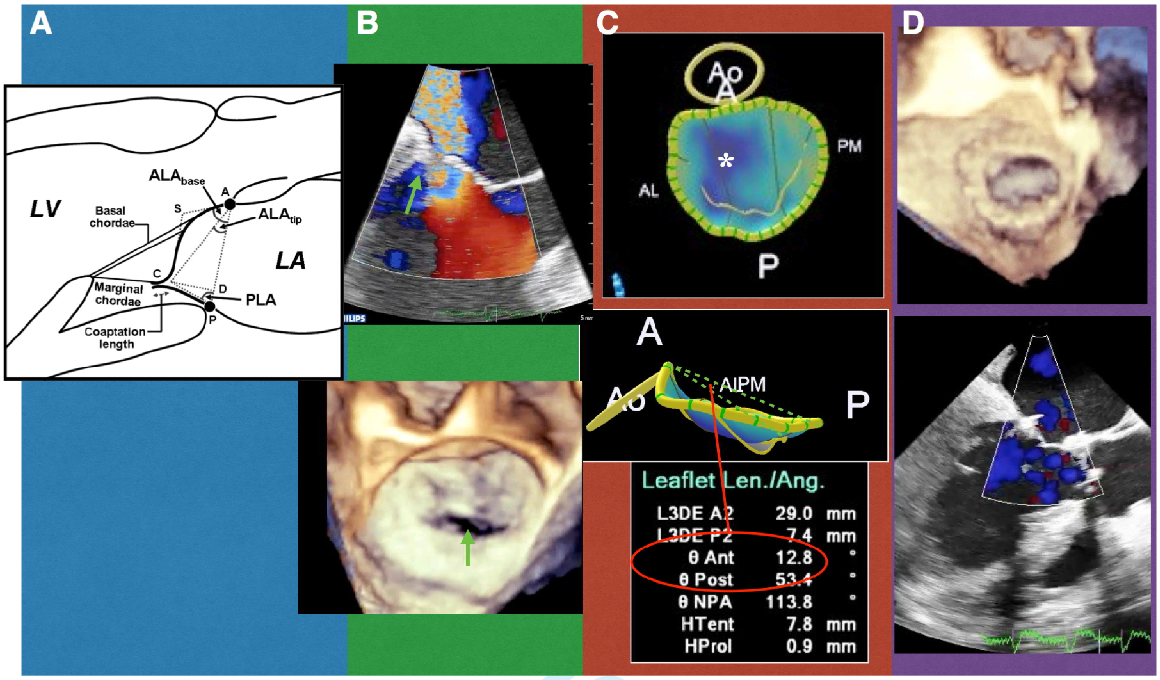
A
B
C
D
LV
LA
ALAbase
ALAtip
Basal chordae
Marginal chordae
Coaptation length
PLA
Ao
A
P
AL
PM
AlPM
Leaflet Len./Ang.
L3DE A2 29.0 mm
L3DE P2 7.4 mm
θ Ant 12.8 °
θ Post 53.4 °
θ NPA 113.8 °
HTent 7.8 mm
HProl 0.9 mm

Figure 6

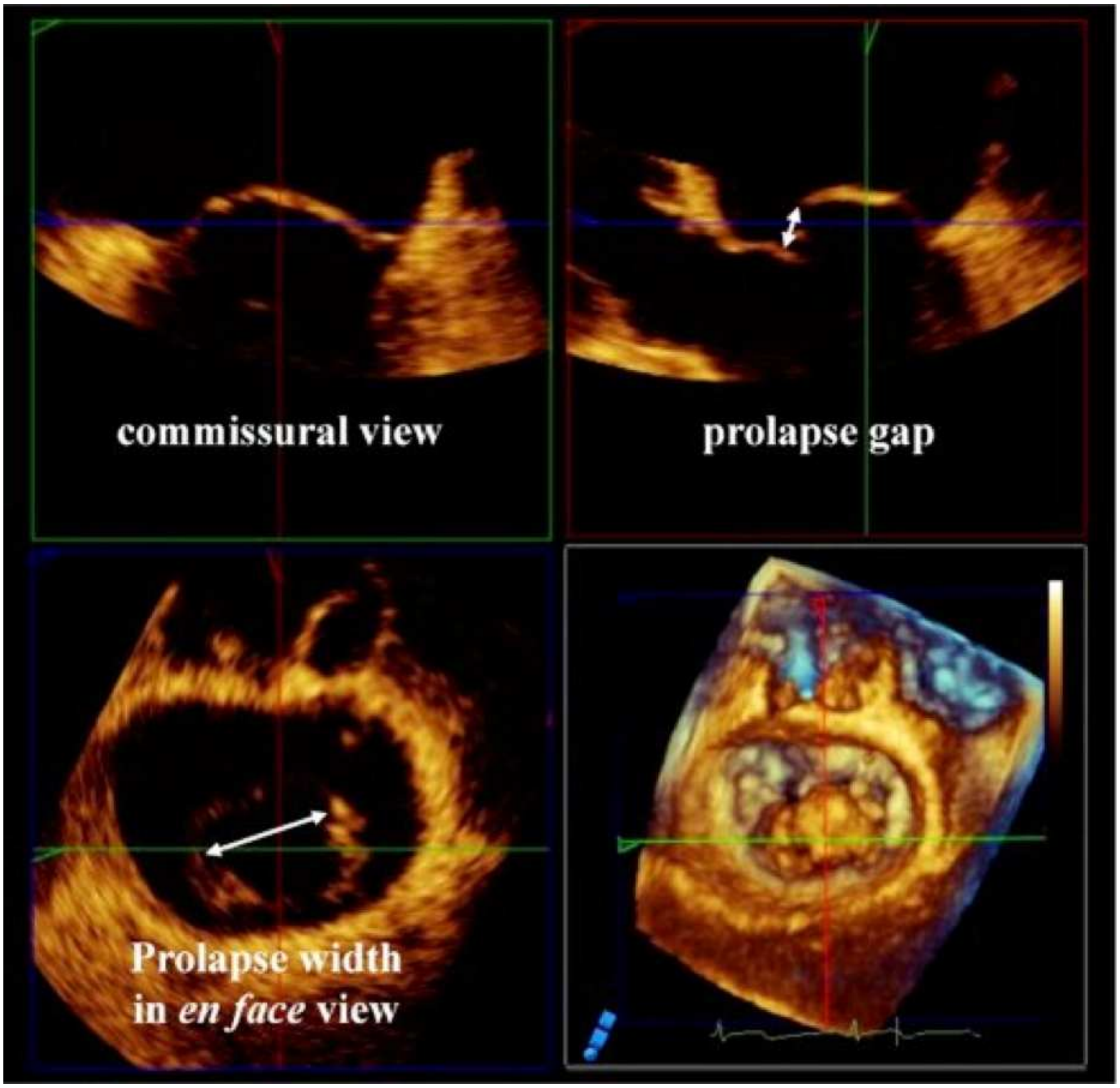
commissural view
prolapse gap
Prolapse width
in *en face* view